Limnol. Oceanogr., 50(6), 2005, 1989–1998

Particle depletion above experimental bivalve beds: In situ measurements and numerical modeling of bivalve filtration in the boundary layer

Per R. Jonsson
Tjärnö Marine Biological Laboratory, Department of Marine Ecology, Göteborg University, SE-452 96 Strömstad, Sweden

Jens K. Petersen
The National Environmental Research Institute, P.O. 358, DK-4000 Roskilde, Denmark

Örjan Karlsson and Lars-Ove Loo
Tjärnö Marine Biological Laboratory, Department of Marine Ecology, Göteborg University, SE-452 96 Strömstad, Sweden

Stefan Nilsson[1]
Department of Naval Architecture and Ocean Engineering, Chalmers University of Technology, SE-412 96 Göteborg, Sweden

Abstract

Suspension feeders may deplete the near-bed layer of food particles, limiting growth of downstream individuals. In a field experiment, we examined food depletion above a bed with bivalves (*Cerastoderma edule*) compared to beds devoid of suspension feeders and how depletion depended on boundary-layer flow. Water above the test plots was sampled with an array of artificial siphons mimicking bivalve inhalant flow. Along the 3-m bed with bivalves, chlorophyll *a* (Chl *a*) in the near-bed layer was depleted by 5–30%. Contrary to expectations from turbulent mixing, Chl *a* depletion increased with friction velocity. To explore the possibility that the bending of the exhalant jet in a strong boundary-layer flow could lead to this depletion, we studied the advection and turbulent diffusion of exhalant water by the injection of fluorescent dye through artificial siphons. The plume of fluorescent dye indicated that the interaction between the exhalant jet and horizontal water flow strongly affected the near-bed mixing of depleted water. At high ratios between jet and friction velocities (VR), the vertical momentum of the exhalant jet reduced the proportion of exhalant water reaching downstream neighbors. A hydrodynamic model incorporating inhalant and exhalant flows in the boundary layer predicted that exhalant jet flow lines reach the bed immediately downstream when the VR ratio is <20, potentially increasing refiltration at higher flow speeds due to jet bending. However, the model could not reproduce the observed increase in refiltration with increasing friction velocity in simulations of aggregated filtration in a bed of bivalves.

There is a strong sense that beds of benthic suspension feeders have a profound effect on water column characteristics (Petersen 2004) and that the removal of suspended particles also has implications for ecosystem functions such as water visibility (Cloern 1982), bloom formation (Koseff et al. 1993), nutrient regeneration (Asmus and Asmus 1991; Dame 1996), oxygen deficiency (Jørgensen 1980), and sediment erosion (Paterson and Black 1999). Benthic suspension-feeders can thus act as a filter with respect to eutrophication of shallow estuaries (Cloern 2001). Dense beds of suspension-feeding bivalves, e.g., blue mussels (*Mytilus edulis*), cockles (*Cerastoderma* spp.), and clams (*Mya arenaria*) have been shown to have the potential to clear the water column of particles on time scales of <1 d (Cloern 1982; Muschenheim and Newell 1992; Petersen et al. 2002).

The activity of benthic suspension feeders has been shown to result in a near-bed layer depletion of particles (Wildish and Kristmanson 1979; Fréchette et al. 1989; Dolmer 2000). Elaborate laboratory studies of flume flow have demonstrated that, under realistic flow regimes, a concentration boundary layer may build up, indicating significant refiltration in dense bivalve beds (Monismith et al. 1990; O'Riordan et al. 1995; Sobral and Widdows 2000). The coupling between water column seston and benthic suspension feeding is, however, still poorly understood, particularly in quantitative and predictive terms (e.g., Koseff et al. 1993; Petersen 2004). The impact of dense beds of bivalves, i.e., the realization of the benthic grazing potential, will depend on the mixing characteristics of the area investigated.

Another aspect of the formation of a particle-depleted near-bed layer is that the growth rate for downstream indi-

[1] Present address: Center for Applied Scientific Computing, Lawrence Livermore National Laboratory, Box 808, L-365, Livermore, California 94551, USA.

Acknowledgments

Constructive criticism from three anonymous reviewers and the associate editor is greatly acknowledged. This research is part of the MAST-III/ELOISE project ''Physical forcing and biogeochemical fluxes in shallow coastal ecosystems (PhaSE)'' and is funded through the European Union DG12 (contract MAS3-CT96-0053). This project is partly financed by Tjärnö Centre of Excellence through the European Union, The European Regional Development Fund (ERDF). Additional support for the study was provided to P.R.J. by the Swedish Research Council through contract 621-2002-4770 and by the Hasselblad Foundation. This paper is contribution 502/7 to the EU program ELOISE.

viduals may be affected. Bivalves are dependent on the flow of water to supply them with food, i.e., they are hydrodynamically limited (Wildish and Kristmanson 1997). Food depletion is thus hypothesized to be a key factor explaining spatial patterns of growth rate and bed geometry (Peterson and Black 1987; Herman et al. 1999). Improved predictions of food limitation and spatial variability in the production of suspension feeders will require better models based on a mechanistic understanding of how individual feeding characteristics interact with food composition and near-bed flow. For bivalves, it is of particular interest how the exhalant current is mixed in the boundary-layer flow and how this controls the refiltration proportion for downstream individuals.

To our knowledge, no study has yet investigated food depletion and the mixing of exhalant water under field conditions with often unsteady flow and complex bed roughness. Previous studies have focused either on correlative field measurements in order to test for the presence of near-bed food depletion (Wildish and Kristmanson 1984; Muschenheim and Newell 1992; Dolmer 2000) or on laboratory experiments with the objective of describing the mechanisms involved in the development of a food-depleted near-bed layer (O'Riordan et al. 1993, 1995). The objective of this study was to better understand how siphon flow affects refiltration for downstream individuals under field conditions. This was achieved by combining field experiments using food depletion in a manipulated bed of the bivalve *Cerastoderma edule* with field studies of the distribution of fluorescently marked exhalant water using artificial siphons. Data are then interpreted using a numerical model that explicitly solves for the concentration field around inhalant and exhalant siphons as a function of friction velocity and siphon flow.

Materials and methods

Study site—Field experiments were carried out in a narrow channel between the islands of Tjärnö and Saltö close to the Tjärnö Marine Biological Laboratory (58°53′N, 11°8′E). The channel is 100 m long and ca. 8 m wide with a maximum depth of 0.5–1.5 m, depending on tide, wind, and air pressure. The tidal amplitude is only ca. 0.3 m, and geostrophic and wind-forced flows also contribute significantly to the water current through the channel. The channel bed consists of sandy sediment with dead bivalve shells and low densities of the cockle *C. edule* (Linneaus 1758) and the clam *M. arenaria* Linneaus 1758.

Experimental plots—To study the effect of bivalve suspension-feeding on the near-bed concentration of chlorophyll *a* (Chl *a*), the density of *C. edule* was manipulated in a 3- × 1-m plot located in the middle and parallel to the channel. The density in the experimental plot was increased to 540 individuals m^{-2}, which is a high density but typical of many patches of *C. edule* (André and Rosenberg 1991). To make sure that an upstream control was available regardless of flow direction in the channel, two control plots (3 × 1 m) without *C. edule* were marked on either side of the experimental plot at a distance of 1.5 m (Fig. 1A). After the experiments, three subsamples of 0.1 m^2 each were removed from the plots, and the number, size, and weight of the cockles were determined. The average shell length of the *C. edule* population in the experimental plot was 32 ± 4.5 mm (mean ± SD, $n = 100$) and the tissue dry weight (dried at 60°C for 24 h) was 1.4 ± 0.23 g (mean ± SD, $n = 100$).

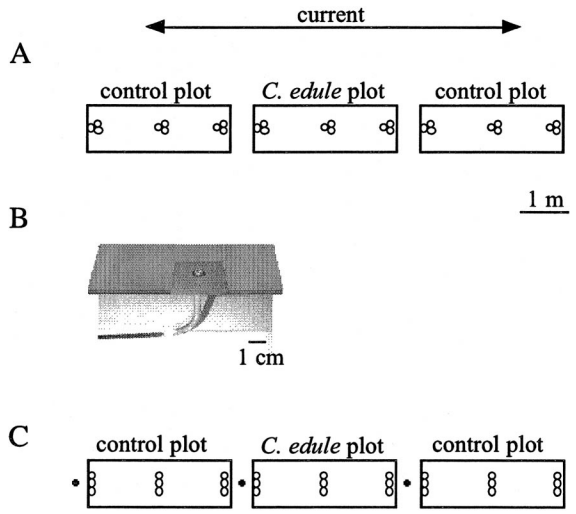

Fig. 1. (A) Schematic drawing of relative positions of the experimental plots and artificial siphons collecting water for Chl *a* measurements. In each group of siphons (5 cm within-group distance), the three siphons were adjusted to a height of 0–0.5, 2, and 8 cm above the bed, respectively. From all siphons, plastic tubes were connected to a bank of peristaltic pumps on shore. (B) Close view of an artificial siphon buried in the sediment. (C) Positions of the experimental plots and artificial siphons for the experiments with the release of fluorescently marked exhalant water. The filled circles in front of each test plot represent the siphons releasing the fluorescent dye. The open circles within the test plots represent inhalant siphons (20 cm within-group distance) collecting water from a height of 0–0.5 cm above the bed.

Near-bed Chl a—Samples were collected from the upstream control and the cockle plots by pumping seawater through artificial siphons with an opening diameter of 3 mm, similar to the inhalant opening of *C. edule* (Fig. 1B). The siphon support with the collecting tube was buried in the sediment with only the siphon protruding. Along the midline of each test plot, three groups of artificial siphons were placed at the leading, middle, and trailing edges, respectively (Fig. 1A). The three siphons in each group were adjusted to open 0–0.5 (natural height), 2, and 8 cm above the seabed, where 0–0.5 cm was regarded as flush with the sediment (considering the roughness of the bed). Above each test plot, one siphon was attached to a buoy 50 cm above the bed. The polyethylene tubes (diameter: 3 mm, length: <20 m) were buried in the sediment to avoid interference with the flow. All tubes were brought to the shore, where they were connected to peristaltic pumps. The pumping rate through each siphon was ca. 50 mL min^{-1}, which is similar to the water-processing rate of a large *C. edule* (André et al. 1993). Simultaneous samples from all the siphons in the experimental plot with *C. edule* and the siphons in the upstream control plot were collected for 6 min (ca. 300 mL), discarding more than the initial 100 mL that represents the tube

Table 1. All experimental series and the measured flow conditions (some series share flow measurements). Flow speed is given as the result of *x, y,* and *z* components at a height above the bed of 20 cm, except for 24 November, which refers to a height of 10 cm. RMS is the standard deviation of the resultant flow speed over a 3-min sampling period (25 Hz). Friction velocity (u_*) was calculated from average Reynolds stress at the heights of 4 and 8 cm (*see Eqs. 2, 3*). Dates refer to the year 1998.

Experimental series	Samples (No.)	Date	Flow speed (cm s^{-1})	RMS (cm s^{-1})	u_* (cm s^{-1})	Time (hh:mm)
Chl *a* reduction	20	4 Sep	17.3	2.94	1.15	10:00
						10:30
			20.4	3.45	1.19	11:50
						12:20
			20.6	3.71	1.75	13:00
						13:30
						14:00
						14:30
			26.0	4.00	2.01	14:50
						15:20
			29.3	4.49	2.04	16:00
						16:30
		5 Sep	19.9	3.90	1.19	9:50
						10:20
						10:40
			19.9	3.90	1.31	11:00
		6 Sep	16.6	2.77	0.89	6:50
						7:20
						7:40
			13.6	2.63	0.46	8:00
						8:30
						9:00
						9:20
			8.70	1.80	0.68	9:50
						10:20
						10:40
		7 Sep	10.8	1.77	0.74	18:50
						19:20
			7.10	1.31	0.87	20:00
						20:30
Dye release	27	10 Sep	22.0	4.30	1.64	13:50
						14:30
			27.5	4.73	2.06	15:10
						15:40
						17:00
Dye release, local	28	18 Nov	4.40	0.67	0.30	13:50
	12	24 Nov	5.00	0.65	0.45	14:00

volume (error of between-sample contamination was <10%). Immediately after collection, a subsample of 100 mL from each siphon was first prefiltered through a 100-μm sieve to remove zooplankton and macrophyte parts. The sample was then filtered through a GF/C filter, soaked in 10 mL of 96% ethanol, and placed in a cool, dark location for 24 h. After extraction in ethanol, the Chl *a* content was measured fluorometrically (Turner Design 450). Fluorescence units were converted to weight of Chl *a* (μg L^{-1}) by correlation with standards. For 4 d, 30 series of samples from each siphon were collected (a total of 600 samples, *see Table 1*).

Release of fluorescent dye in the near-bed layer—To explore the effect of bending of the exhalant jet in the boundary-layer flow, we performed a series of field experiments in which advection and turbulent diffusion of bivalve exhalant water in the near-bed layer was mimicked. The general design in these experiments involved the injection of fluorescently marked seawater through an artificial siphon and downstream sampling of the plume of the fluorescent marker. Fluorescently marked seawater was prepared by dissolving ca. 1 g of either rhodamine B or fluorescein in 2.5 liters of near-bed seawater and keeping this at field temperature to minimize density differences.

In the first series of experiments, one dye-injection siphon was mounted with its opening 0–0.5 cm above the sediment 25 cm upstream of the first control plot and connected to a peristaltic pump on shore with a 20-m polyethylene tube (Fig. 1C). The tube diameter was 3 mm (similar to cockle exhalant openings), and injection rates ranged from 26 to 54 mL min^{-1}, which give realistic exhalant velocities for *C. edule.* A second injection siphon was placed 25 cm upstream of the experimental plot with *C. edule,* and a third injection

siphon was placed 25 cm upstream of the second control plot. The first and third siphons injected water marked with rhodamine B, and the second siphon (*C. edule* plot) released water with fluorescein (Fig. 1C). The use of two separate dyes prevented contamination from the first to the second plume, and when the first rhodamine B plume encountered the second control plot, its concentration was two orders of magnitude lower than in the second downstream plume of rhodamine B. The uncontaminated fluorescein plume could be monitored along two test plots for a total of 6.75 m. In each test plot, nine artificial siphons collected water at a height of 0–0.5 cm above the sediment as described above. The nine siphons were distributed in three groups placed at the leading, middle, and trailing edge, respectively. In each group, one siphon was placed at the test plot midline, and the two others on each side of the midline were placed at a distance of 20 cm (Fig. 1C). To ensure sampling of the plume core, which varied slightly in direction on short time scales, the sample with the maximum concentration at each distance was selected for analysis of turbulent diffusion (Eq. 1). Collection of near-bed water was set to ca. 50 mL min^{-1} and carried out as described for the Chl *a* samples above. This was repeated five times, making a total of 135 samples (Table 1).

The experiments described above on the distribution of an exhalant plume only considered distances between exhalant and inhalant siphons >25 cm. In many natural populations of *C. edule*, adjacent individuals may be considerably closer. To investigate local effects of the flow-induced bending of the exhalant jet, a second series of experiments was performed. Four artificial siphons that collected water 0–0.5 cm above one of the control plots were placed 6, 11.5, 16.3, and 25.5 cm downstream of the siphon injecting a fluorescent marker (fluorescein). Water was collected as described above, and the experiment was repeated three, four, and three times with injection rates of 54, 29, and 26 mL min^{-1}, respectively (40 samples, Table 1). These flow rates correspond to jet velocities between 6 and 13 cm s^{-1}. As suggested by O'Riordan et al. (1995), the downstream distribution of the exhalant water was plotted as a function of the ratio between the exhalant jet speed and the friction velocity and was termed the velocity ratio (VR). The concentrations of fluorescent markers in all samples were measured on a spectrofluorometer (Shimadzu RF-510) using excitation wavelengths of 546 and 494 nm and recording emission at 578 and 520 nm for rhodamine B and fluorescein, respectively. To describe the plume of exhalant water, a plume model for a point source in a boundary layer was used (Okubo 1980):

$$C_{(x,y,z)} = \frac{2Q}{\pi U c_y c_z x^{2-n}} e^{-x^{n-2}[(y^2/c_y^2)+(z^2/c_z^2)]} \quad (1)$$

where $C_{(x,y,z)}$ is the concentration downstream located in space by the Cartesian coordinates *x*, *y*, and *z*; *Q* is the emission rate of the exhalant water; *U* is the flow speed; and c_y, c_z, and *n* are empirical constants. From the data on the distribution of exhalant fluorescent marker obtained from the field experiments, the constant *n* was fitted from the slope of the logarithmic concentration against the logarithmic distance. The constants c_y and c_z were coarsely fitted to the initial width of the plume (estimated with a ruler 0–3 m downstream) and given the values 0.3 and 0.4, respectively. The fit to experimental data was excellent for distances >0.25 m (*see* ''Discussion'' for deviations close to the exhalant jet).

Flow measurements—At regular intervals during the collection of seawater samples from the artificial siphons, the instantaneous flow speed was measured with an acoustic Doppler velocimeter (ADV; Nortek AS). The ADV probe measures all three velocity components in an active volume (ca. 6 × 6 × 6 mm^3) located 5 cm below the receivers. Velocity measurements were recorded by a computer (sampling frequency: 25 Hz) and corrected for temperature and salinity. The ADV probe was mounted on a vertical steel pole attached to an aluminum tray that was placed on the seabed between the control and experimental plot. The active volume of the ADV probe was initially adjusted to ca. 0.5 cm above the bed, and a 3-min sample of current velocity was collected. This was then repeated to obtain flow speeds from six heights up to 20 cm above the bed. To obtain measurements within a short time interval, friction velocity was calculated from the Reynolds stress (τ_R) as:

$$u_* \approx \sqrt{\frac{\tau_R}{\rho}} \quad (2)$$

where ρ is the seawater density. Reynolds stress was calculated from the correlation between the turbulent velocities u' and w' as:

$$\rho_R = \overline{u'w'}\rho \quad (3)$$

Reynolds stress was similar at 4 and 8 cm above the bed, which is 5–10% of the boundary-layer thickness, indicating that there is a constant stress layer (Schlichting 1979) and that Reynolds stress dominated the total stress. When comparisons were possible (steady flow conditions), the friction velocities were also estimated from the velocity gradient in the logarithmic layer according to Schlichting (1979):

$$u_z = \frac{u_*}{\kappa} \ln\left(\frac{z}{z_0}\right) \quad (4)$$

where u_z is horizontal velocity at depth *z*, z_0 is the roughness height, and κ is the von Karman's constant (0.4). Estimates of friction velocity from Reynolds stress and from the velocity gradient showed good agreement.

Model of refiltration in beds of C. edule—In an attempt to test the hypothesis that increasing the bending of the inhalant jet at higher boundary-layer flow speeds caused enhanced refiltration in beds of *C. edule*, we formulated a hydrodynamic model based on the Reynolds averaged Navier–Stokes (RANS) equation for the siphon velocity field in a turbulent boundary layer and an advection-diffusion equation. Initially, a fully three-dimensional model was formulated, but the numerical solutions were too demanding in terms of computational power requirements. Instead, the advection-diffusion equation describes the two-dimensional concentration field (in the x–z-axes) of a particulate, neu-

trally buoyant marker advected by the velocity field along a bed of *C. edule* of infinite width (along the y-axis). The Reynolds average of a quantity u is the same as the time average for our purposes and is designated with a capital U. The RANS equation is (e.g., Tennekes and Lumley 1972):

$$\frac{\partial U_i}{\partial t} + U_j\frac{\partial U_i}{\partial x_j} = -\frac{1}{\rho}\frac{\partial P}{\partial x_i} + \frac{\partial}{\partial x_j}\left(\nu\frac{\partial U_i}{\partial x_j} - \overline{u_i' u_j'}\right)$$

$$\frac{\partial U_i}{\partial x_i} = 0 \qquad (5)$$

Here, U_i is the velocity component along the x_i-axis ($x_1 = x$, $x_2 = z$), ρ is the water density, ν is the kinematic viscosity, and $-\overline{u_i' u_j'}$ is called the specific Reynolds stress tensor. The specific Reynolds stress tensor needs to be modeled. Here, a nonlinear k-ε-model was used, resulting in two extra equations to solve simultaneously with the RANS equation (Craft et al. 1996). The influence of cockles on the boundary layer flow entered the model as boundary conditions for Eq. 5. The siphonal openings were modeled as parabolic inflow and outflow profiles on the bottom with the exhalant siphon 1.8 cm downstream of the inhalant siphon. To obtain a realistic boundary-layer profile, the flow was modeled for a length of 0.5 m in front of the leading edge of the bivalve bed.

The cockles are assumed to clear the fluorescent marker from the water with 100% efficiency. Advection is computed using the obtained Reynolds averaged velocity field. The time course of advection over the length of the cockle bed is considered sufficiently short to ignore internal sources and sinks of the particulate marker. On the basis of the assumptions above, the balance between advection and turbulent diffusion is described as follows:

$$\frac{\partial C}{\partial t} + U_j\frac{\partial C}{\partial x_j} = \frac{\partial}{\partial x_j}\left(\Gamma\frac{\partial C}{\partial x_j}\right) - \frac{\partial}{\partial x_j}(\overline{u_j' c'}), \qquad (6)$$

where Γ is the diffusion constant, the turbulent mass flux $\overline{u_j' c_j}$ accounts for the extra transport of C due to turbulence, and C is the Reynolds averaged mass concentration of the marker. The turbulent mass flux is modeled as follows:

$$\overline{u_j' c'} = -\Gamma_\tau\frac{\partial C}{\partial x_j}, \qquad (7)$$

where Γ_τ is the turbulent diffusion and can be obtained from the k-ε-model. The partial differential equations (Eqs. 5, 6), including the extra turbulence equations, were discretized over a two-dimensional domain, including the bivalve bed, using finite difference methods and were solved numerically. The model was solved using parallel computing on an IBM SP with multiple computational nodes (16 processors per node). A description of the software used in the discretization and solution step can be found in Nilsson (2002). In a series of simulations, we explored the effects of friction velocity (0.001–0.04 m s^{-1}), exhalant jet velocity (0.025–0.1 m s^{-1}), and bivalve density (intercockle distance: 0.05 and 0.1 m) on both local effects (reattachment distance of flow lines) and aggregated refiltration along the bed.

Statistical methods—If not otherwise indicated, data are reported in the text, tables, or figures as means with a 95% confidence interval. Analysis of variance (ANOVA) was used to test for differences in Chl *a* and the % reduction of Chl *a*. Changes in Chl *a* concentration were tested in a three-factor ANOVA, with the plot type and distance from the leading edge as fixed factors and the date as a random factor. In a two-factor ANOVA for each date, we tested for differences in % Chl *a* reduction with the plot type and height above the bed as fixed factors. Tests for homogeneity of variances were performed using Cochran's test (Underwood 1996). Tests of correlation between Chl *a* depletion and friction velocity were performed with the nonparametric Spearman's correlation. In all tests, a type I error (α) of 0.05 was used.

Results

Flow regime—The water current through the channel flowed north during all experiments, although the speed varied on short time scales. The velocity profile in the near-bed layer was approximately logarithmic on most occasions ($r^2 > 0.9$). Table 1 shows a summary of the ADV measurements and calculations of root-mean-square (RMS) and friction velocity (u_*) for the sample occasions. During the measurements of Chl *a* depletion the flow speed at a height of 20 cm varied between 7 and 30 cm s^{-1} (u_* = 0.9–2 cm s^{-1}), and during the experiments with the release of fluorescent markers, the flow speed varied between 1.5 and 27 cm s^{-1} (u_* = 0.25–2.1 cm s^{-1}). RMS and friction velocity were ca. 20% and 7% of the velocity at a height of 20 cm, respectively.

Near-bed Chl a—The Chl *a* concentration was ca. 1 μg L^{-1} throughout the experimental study, and no marked difference between near-bed concentrations and the bulk water at 50 cm was detected at the control plot (data not shown). Table 2 shows the near-bed Chl *a* concentrations for the control and the experimental plot stocked with *C. edule* (540 m^{-2}). Estimated concentrations of Chl *a* are given for three distances downstream from the leading edge of each test plot and for three heights above the bed. Over all dates, there was a significant interaction for Chl *a* concentration between plot type and distance from leading edge (three-factor ANOVA, $F_{2,6} = 5.7$, $p < 0.05$), demonstrating a reduction in Chl *a* over the experimental plot with *C. edule*.

Chl *a* concentration and flow conditions changed over time scales of some hours, adding variability to replicates within 1 d and among dates. To improve the power of the test for the near-bed depletion of Chl *a* above the experimental plot with *C. edule*, we calculated the reduction in Chl *a* from the leading to the trailing edge for each replicate in each test plot. Over the 3-m length of the experimental plot containing *C. edule*, the near-bed concentration of Chl *a* decreased significantly more than over the control plot without bivalves on 4, 6, and 7 September 1998 (two-factor ANOVA, $F_{1,66} = 73.5$, $F_{1,54} = 8.95$, $F_{1,18} = 34.2$, $p < 0.05$,), while on 5 September, this effect was significant only at an 8-cm height above the bed (two-factor ANOVA, $F_{2,7} = 5.15$, $p < 0.05$). Statistically significant depletion rates of Chl *a* above the experimental plot were between 5 and 30% (Fig. 2) and differed significantly from depletion above control plots

Table 2. Chlorophyll *a* concentrations (μg L^{-1}, mean ± SD) for the upstream control plot without bivalves and the experimental plot with *Cerastoderma edule* (540 ind. m^{-2}). Samples were collected on four dates in 1998 from the leading edge, from the middle (1.5 m), and at the trailing edge (3 m) of each plot and at three heights (0.5, 2, and 8 cm) above the bed (data from 50-cm height are not shown).

		Control plot			*C. edule* plot		
Date	Bed position	0.5 cm	2 cm	8 cm	0.5 cm	2 cm	8 cm
4 Sep	Leading	1.17 ± 0.18	1.12 ± 0.18	1.13 ± 0.18	1.16 ± 0.20	1.17 ± 0.20	1.48 ± 0.18
$n = 12$	Middle	1.16 ± 0.19	1.16 ± 0.20	1.10 ± 0.17	1.20 ± 0.19	1.10 ± 0.19	1.10 ± 0.14
	Trailing	1.23 ± 0.16	1.13 ± 0.17	1.12 ± 0.16	1.07 ± 0.23	1.00 ± 0.18	1.05 ± 0.20
5 Sep	Leading	0.85 ± 0.08	0.84 ± 0.06	0.87 ± 0.07	0.86 ± 0.06	0.86 ± 0.05	0.90 ± 0.05
$n = 4$	Middle	0.90 ± 0.07	0.83 ± 0.05	0.88 ± 0.03	0.72 ± 0.20	0.83 ± 0.04	0.81 ± 0.06
	Trailing	0.86 ± 0.04	0.84 ± 0.06	0.87 ± 0.06	0.83 ± 0.04	0.85 ± 0.04	0.84 ± 0.05
6 Sep	Leading	0.81 ± 0.08	0.78 ± 0.03	0.78 ± 0.04	0.80 ± 0.07	0.82 ± 0.04	0.85 ± 0.07
$n = 10$	Middle	0.79 ± 0.08	0.78 ± 0.06	0.82 ± 0.09	0.76 ± 0.10	0.80 ± 0.06	0.82 ± 0.04
	Trailing	0.80 ± 0.08	0.80 ± 0.04	0.78 ± 0.08	0.76 ± 0.08	0.77 ± 0.06	0.80 ± 0.07
7 Sep	Leading	0.71 ± 0.13	0.71 ± 0.06	0.76 ± 0.07	0.69 ± 0.06	0.78 ± 0.05	0.86 ± 0.06
$n = 4$	Middle	0.74 ± 0.04	0.75 ± 0.03	0.78 ± 0.02	0.62 ± 0.02	0.70 ± 0.02	0.78 ± 0.01
	Trailing	0.72 ± 0.04	0.75 ± 0.02	0.83 ± 0.03	0.64 ± 0.04	0.65 ± 0.04	0.74 ± 0.03

(two-factor ANOVA, $F_{1,172} = 59.4$, $p < 0.05$), except on 5 September. Depletion of Chl *a* was significantly less at the sampling depth of 0–0.5 cm above the experimental plot than at 2 and 8 cm on 4 September (one-factor ANOVA, SNK, $F_{2,33} = 15.4$, $p < 0.05$).

Unexpectedly, a positive correlation (Spearman's correlation, $z = 2.36$, $p < 0.05$) was found between friction velocity (u_*) and Chl *a* depletion (Fig. 3). This observation was puzzling, since the increase in turbulent diffusion is expected to reduce Chl *a* depletion along the cockle bed through vertical mixing. The empirical studies of the exhalant jet flow and the numerical model, presented and discussed below, were included to explore possible explanations for this positive correlation between friction velocity and Chl *a* depletion.

Near-bed dilution of fluorescent markers—The interaction between the exhalant jet flow from an artificial siphon and the near-bed flow resulted in a plume advected downstream along control plot 1, the experimental plot stocked with *C. edule,* and control plot 2. The slope of the decreasing proportion of exhalant dye concentration with distance was fitted to Eq. 1 and represents the rate of turbulent diffusion. An example is shown in Fig. 4 (filled symbols). The average slopes were −1.77 ± 0.05, −1.66 ± 0.2, and −1.25 ± 0.18 for the *C. edule* and the control plots 1 and 2, respectively.

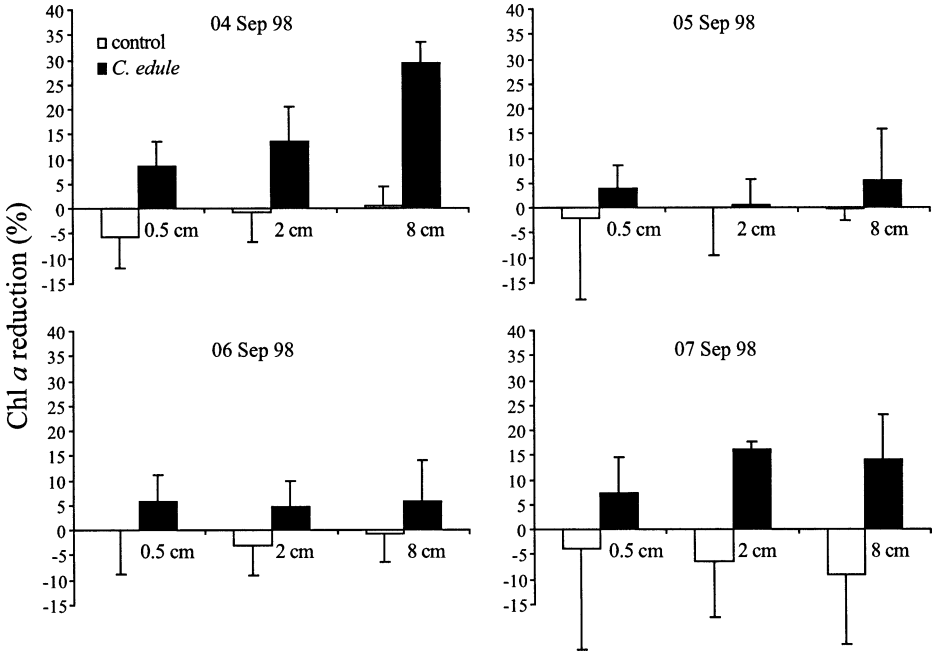

Fig. 2. Calculated reduction of Chl *a* (%) over the length (3 m) of the upstream control and *C. edule* plots for all dates and all sample heights above the bed. Sample sizes are 12, 4, 10, and 4 for 4, 5, 6, and 7 September, respectively.

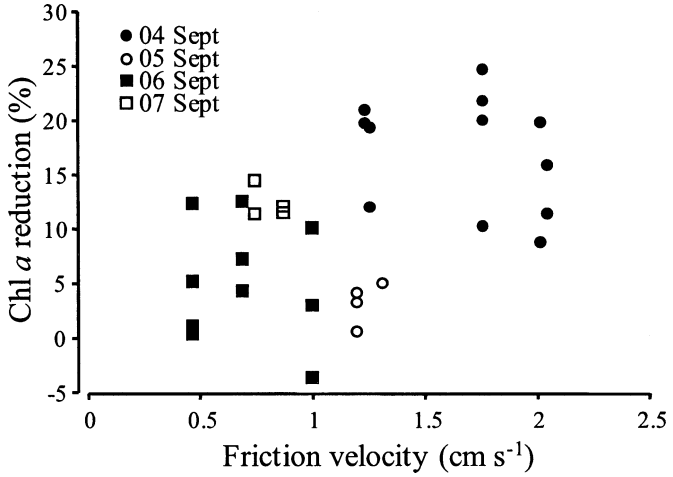

Fig. 3. Chl *a* reduction (%) over the experimental plot stocked with *C. edule* as a function of the friction velocity (cm s^{-1}). Data on Chl *a* reduction were averaged over all three sample heights.

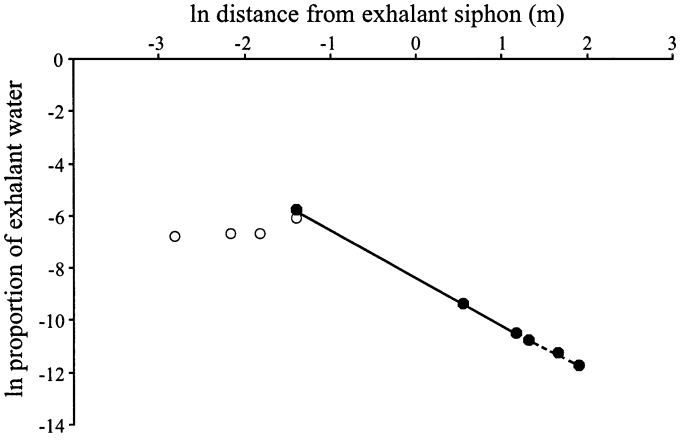

Fig. 4. Plot of the logarithm (ln mean, $n = 5$ for filled circles and $n = 3$ for open circles) of concentration of the fluorescein marker of exhalant water as a function of the logarithm of distance downstream from the exhalant siphon. The concentration of the marker is expressed as the proportion of the concentration released from the exhalant siphon and sampled with the downstream siphons in the middle of the test plots. The two lines represent fits to the plume equation (Eq. 1), with the solid line representing the cockle plot (slope = −1.77) and the dashed line representing the control plot (slope = −1.66). The open circles show concentrations sampled close (<0.25 m) to the exhalant siphon. The friction velocities were 1.64 and 0.45 cm s^{-1} for the filled and open circles, respectively.

Typical slopes for turbulent diffusion of point source plumes are around −1.75 (Okubo 1980).

The second series of experiments focused on the local effect (5–25 cm) of jet bending in the near-bed flow. The concentration of exhalant water close to the release point (Fig. 4, open symbols) was much less than expected from the distribution of exhalant water measured further downstream in the first series of experiments (Fig. 4, filled symbols). Figure 5 shows the strong relation between the concentration of exhalant water sampled and the ratio between exhalant jet speed and friction velocity (VR).

Model of refiltration in beds of C. edule—The numerical model of inhalant/exhalant flow in a turbulent boundary layer produced a clear deflection of the exhalant jet in the boundary-layer flow, seen as a recirculation zone of water on the downstream side of the exhalant jet (Fig. 6). The reattachment distance of exhalant flow lines was used as a measure of possible local refiltration for downstream cockles (Fig. 7). The VR ratios from a range of friction and jet velocities fall on an approximately common curve, and the reattachment distance increased with VR. When the siphon flow of a series of downstream bivalves is simulated, a concentration boundary layer builds up (Fig. 8A). After a short distance downstream from the leading edge of the cockle bed, the fraction of refiltered water reached an asymptotic value (Fig. 8B). As expected, aggregated refiltration increased with cockle density, but in contrast to the observed field data, the model predicted a monotonic decrease in refiltration with friction velocity (Fig. 9).

Discussion

The field experiment where an experimental plot was stocked with the bivalve *C. edule* showed a significant decrease in Chl *a* from the leading edge to the trailing edge, an effect that was absent in a similar control plot without bivalves. This result strongly suggests that the reduction in Chl *a* was caused by the feeding activity of *C. edule*. The statistically significant depletion rates of Chl *a* found in the near-bed layer differed among sampling occasions and were between 5 and 30% over the length of the 3-m plot. It is difficult to compare these rates with other field studies of food depletion because of differences in suspension-feeder

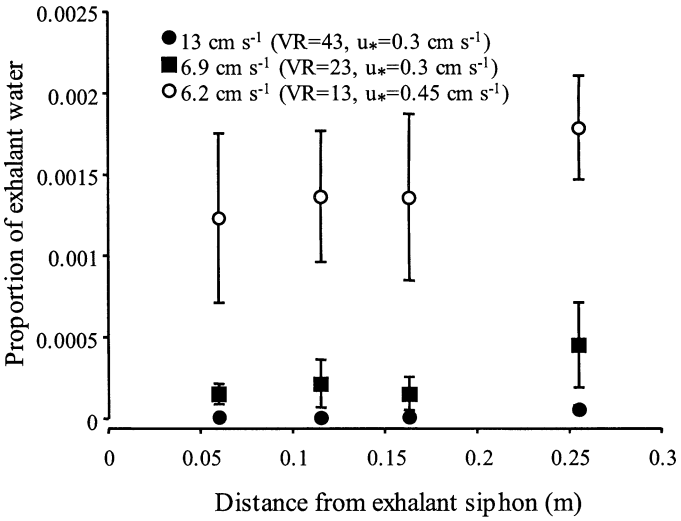

Fig. 5. Concentration (mean ± SE) of fluorescent marker from an exhalant siphon sampled at short distances (6–26 cm) downstream of the source. Concentration is expressed as the proportion of the concentration released from the exhalant siphon. Data are shown for three different ratios between jet velocity and friction velocity (VR). Jet and friction velocities are indicated in the panel as cm s^{-1} ($n = 3$ for VR = 43 and 13, and $n = 4$ for VR = 23).

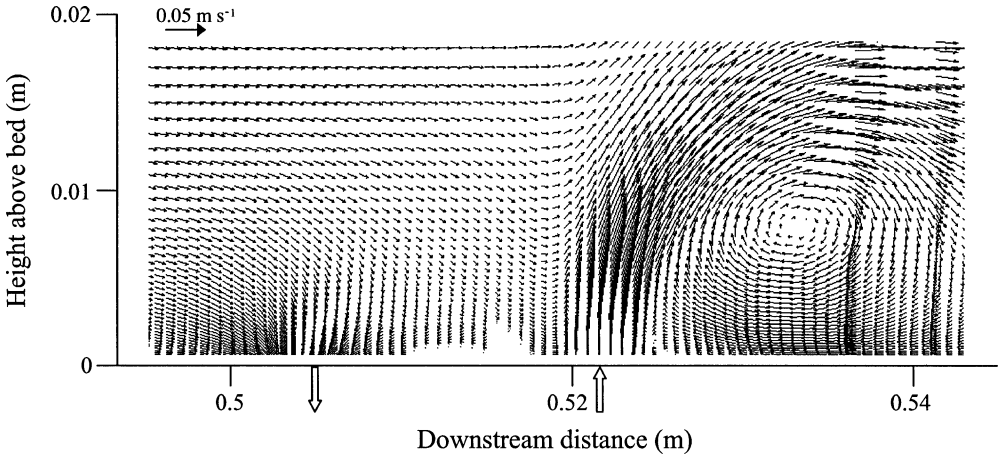

Fig. 6. Time-averaged flow field showing modeled inhalant and exhalant siphon currents interacting with the turbulent boundary-layer flow. The position of the siphons is indicated by the block arrows below the x-axis. Exhalant jet, free-stream, and friction velocities are 0.05, 0.12, and 0.005 m s^{-1}, respectively.

abundance, bed size, height of measurements, and hydrodynamic conditions. Muschenheim and Newell (1992) found a 60–85% depletion of diatoms in near-bed water 11 m downstream in a bed of *M. edulis.* In a Danish fjord, Riisgård et al. (1998) measured a 50% reduction in Chl *a* 400 m downstream over a bed of the ascidian *Ciona intestinalis.* Butman et al. (1994) found a Chl *a* reduction of 60% in slow flow and 45% in fast flow 5.5 m downstream over a *M. edulis* bed in a laboratory flow tank. In an excellent series of experiments, the mixing of exhalant water in the near-bed flow was studied in a flow tank with artificial inhalant and exhalant siphons, mimicking infaunal bivalves (Monismith et al. 1990; O'Riordan et al. 1993, 1995). For siphon configurations similar to *C. edule,* they found that 7–18% of the exhalant water accumulated in the near-bed layer 2.8 m downstream of a bed with 625 siphons m^{-2}. There are also studies in which significant food depletion was not found, often in strong tidal flows (e.g., Roegner 1998). In conclusion, the evidence from our studies and previous studies is

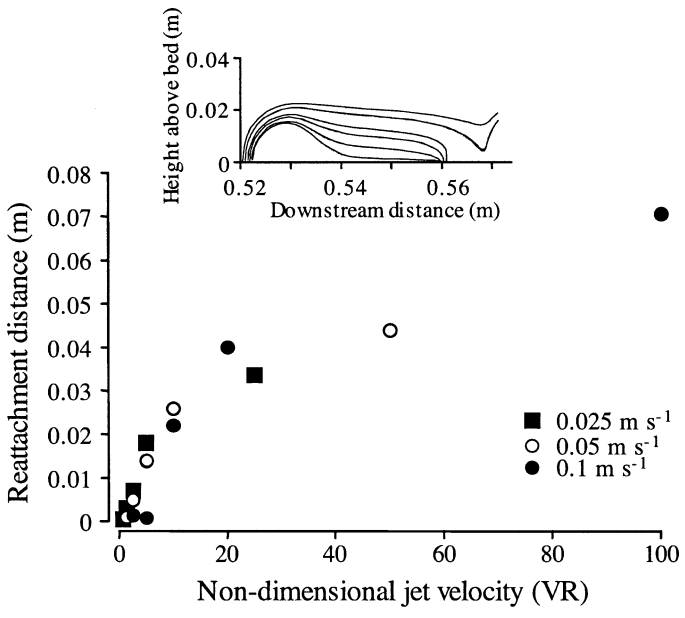

Fig. 7. The downstream distance from the exhalant siphon to the point of modeled flow-line reattachment as a function of the nondimensional jet speed (VR). The legend indicates the absolute jet speeds. The inset shows some flow lines of the deflected exhalant jet in the boundary-layer flow (VR = 10, $u_* = 0.005$ m s^{-1}). The reattachment distance is defined as the distance from the flow line leaving the downstream end of the exhalant siphon to the position where it comes within 1 mm of the bed.

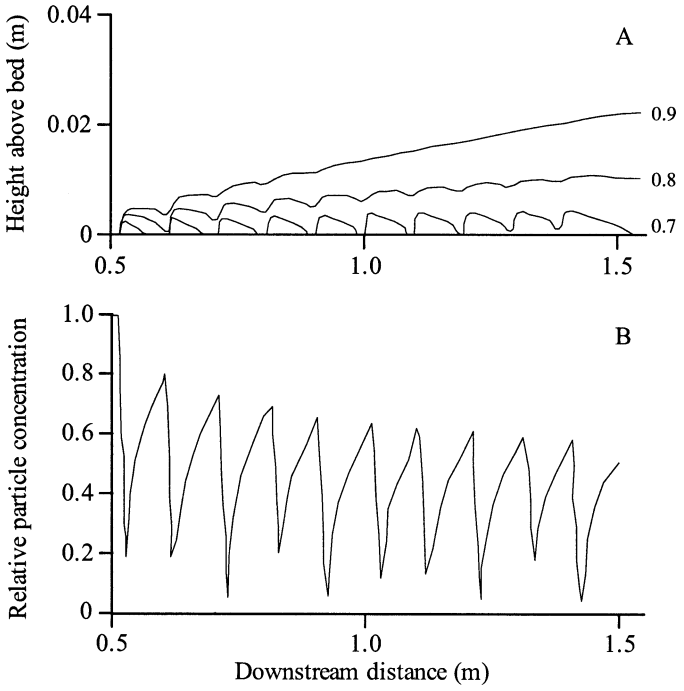

Fig. 8. Modeled concentration boundary layer along a bed of cockles (10 cm between individuals) depicted as (A) downstream isolines of relative particle concentration (bulk concentration = 1) as a function of the height above the bed ($u_* = 0.01$ m s^{-1}) and (B) downstream particle concentration at a height of 0.005 m above the bed ($u_* = 0.01$ m s^{-1}). The exhalant jet velocity is 0.05 m s^{-1}.

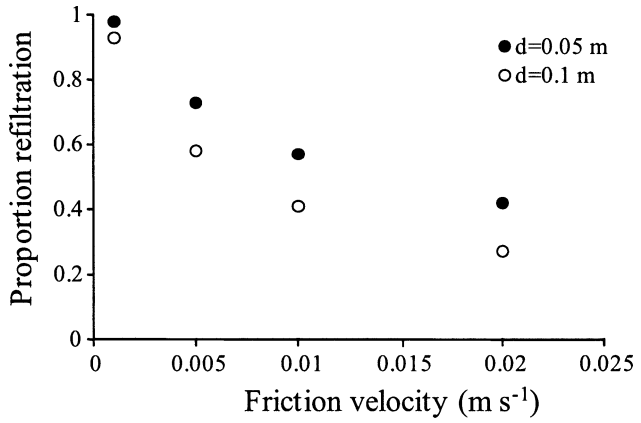

Fig. 9. Proportion of refiltered water as a function of friction velocity over modeled beds of cockles separated with a distance (d) of 0.05 and 0.1 m. Refiltration rate is the near-asymptotic value at the downstream end of the bed. The exhalant jet velocity is 0.05 m s^{-1}.

strong for the presence of near-bed depletion, although the rates differ. Empirical relationships or models are required in these situations to better predict the intensity of food depletion, mainly as a function of flow regime and suspension-feeder density.

Our field results, however, failed to support our expectation that food depletion should be less severe when flow speed increased above a bed of suspension-feeding bivalves. The more intense turbulent mixing should erode the concentration boundary layer of exhalant water (Dade 1993). Instead, we found a positive correlation between food depletion and friction velocity, although this correlation is unavoidably confounded by sampling on different dates (Fig. 3). For some combinations of jet and friction velocities O'Riordan et al. (1993), in a flume study with artificial bivalves, also found that refiltration of depleted water increased with friction velocity (for siphons flush with the bed). They explained that this effect was caused by hydrodynamic bending of the exhalant jets in the boundary-layer flow that expelled food-depleted water into the near-bed layer. The exhalant jet has a vertical momentum when it is injected into the near-bed flow through the siphon. In the near-bed flow, the jet will bend over downstream and undergo turbulent mixing with ambient water. If the jet speed is sufficiently high compared to the boundary-layer flow speed, the exhalant water will initially mix higher up above the bed, reducing refiltration for neighbors immediately downstream. At high bed flow speeds (low VR), the jet flow is deflected downstream in the near-bed layer, potentially increasing the concentration of exhalant water in the near-bed layer. In our experiments with fluorescent markers released from artificial siphons, refiltration was lower close to the release point (Fig. 4, open symbols) than expected from the turbulent diffusion rate measured further downstream. We interpret this result as the effect of the vertical momentum in the jet that expels exhalant water to some height where it passes over the inhalant siphons of close neighbors before it reattaches to the bed. This effect was evident only at a distance less than ca. 0.25 m, after which the exhalant water is inhaled at concentrations declining with distance in accordance with turbulent diffusion of a point source plume (Okubo 1980). Figure 5 shows that local refiltration changed by a factor of about 100 when the ratio was changed between the jet speed and the friction velocity of the flow (VR). O'Riordan et al. (1993) described a reduction in whole-bed refiltration in this range of increasing VR in flume experiments for siphons flush with the bed.

The simulation of our numerical model of exhalant jet flow in a turbulent boundary layer was partly in conflict with the results of the field experiment. Compatible with the field results, the model predicted a rapid decrease in reattachment distance of the exhalant jet (Fig. 7) in the same range of VR where local refiltration has been found to increase (Fig. 5, present study; O'Riordan et al. 1993). However, despite the strong deflection of the jet predicted by the model, the simulated refiltration along a cockle bed decreases monotonically with friction velocity (Fig. 9). Thus, within the parameter space tested, the model does not reproduce the empirical results in the present study or in some of the experiments by O'Riordan et al. (1993). It may be speculated that the relationship between refiltration and friction velocity changes from positive to negative depending on jet penetration into the log layer and bivalve density, as indicated by the results obtained by O'Riordan et al. (1995). In the field, roughness elements may also cause skimming flow (Friedrichs et al. 2000), reducing turbulent mixing of the near-bed layer. The numerical model formulated in the present study solves the Navier–Stokes flow equations (within a parameterized turbulent boundary layer) using parallel code and very powerful computers. This is, to our knowledge, the most advanced attempt to model bivalve siphonal flow. However, the computing task was so demanding that it was not practical to solve the fully three-dimensional case. The two-dimensional representation presented implies that siphons have infinite width along the y-axis. Several known three-dimensional turbulent flow structures observed for siphon flow in the boundary layer can thus not be resolved, e.g., horse-shoe eddies. The two-dimensional model also means that water cannot flow around siphonal jets and that the refiltration rate is likely overestimated by the model. Other features are better reproduced by the model, such as the strong concentration boundary layer in beds of bivalves, at least for low friction velocities (Fig. 8A). The asymptotic refiltration rate is reached at a short distance downstream of the leading edge (Fig. 8B), as also found experimentally by O'Riordan et al. (1993). Large-scale growth of the concentration boundary layer is similar to what is predicted by simpler models previously published, e.g., the advection-diffusion model used by Fréchette et al. (1989).

The main conclusion from the field studies, as well as from previous laboratory experiments, is that the relative strengths of boundary-layer flow and bivalve exhalant currents determine the intensity of refiltration. The exhalant water undergoes rapid mixing in the downstream flow (concentration falls as distance$^{-1.75}$). However, the number of upstream bivalves acting as sources of exhalant water only increases approximately linearly with distance. This implies that the contribution of exhalant water from the nearest upstream neighbor dominates and that local flow phenomena,

e.g., jet bending, may scale up to whole-bed refiltration. However, this occurs only when jet bending (e.g., evident as reattachment distance in Fig. 7) overlaps with interindividual distance, and this is expected only in dense beds where the distance among individuals is less than ca. 20 cm and for a VR <10. The surprising positive correlation between friction velocity and refiltration observed in the present field study and in previous laboratory experiments (O'Riordan et al. 1993) could not be reproduced with our numerical model. It is likely that a fully three-dimensional model is required to determine if the observed interaction between boundary-layer flow and exhalant currents can be simulated using only information about friction velocity and exhalant flow speeds. With an expected rapid increase in computational power, the model presented here will easily be extended to three dimensions and may be used to predict critical bed sizes under a range of flow regimes where refiltration restricts positive growth. This is expected to contribute to an improved understanding of the geometry of natural bivalve beds, an optimization of aquaculture management, and predictions of the turnover of nutrients in coastal areas.

References

ANDRÉ, C., P. R. JONSSON, AND M. LINDEGARTH. 1993. Predation on settling bivalve larvae by benthic suspension-feeders: the rôle of hydrodynamics and larval behaviour. Mar. Ecol. Prog. Ser. **97:** 183–192.

———, AND R. ROSENBERG. 1991. Adult–larval interactions in the suspension-feeding bivalves *Cerastoderma edule* and *Mya arenaria*. Mar. Ecol. Prog. Ser. **71:** 227–234.

ASMUS, R. M., AND H. ASMUS. 1991. Mussel beds—limiting or promoting phytoplankton. J. Exp. Mar. Biol. Ecol. **148:** 215–232.

BUTMAN, C. A., M. FRÉCHETTE, W. R. GEYER, AND V. R. STARCZAK. 1994. Flume experiments on food supply to the blue mussel *Mytilus edulis* L. as a function of boundary-layer flow. Limnol. Oceanogr. **39:** 1755–1768.

CLOERN, J. E. 1982. Does the benthos control phytoplankton biomass in the South San Francisco Bay? Mar. Ecol. Prog. Ser. **9:** 191–202.

———. 2001. Our evolving conceptual model of the coastal eutrophication problem. Mar. Ecol. Prog. Ser. **210:** 223–253.

CRAFT, T. J., B. E. LAUNDER, AND K. SUGA. 1996. Development and application of a cubic eddy-viscosity model of turbulence. Int. J. Heat Fluid Flow **17:** 108–115.

DADE, W. B. 1993. Near-bed turbulence and hydrodynamic control of diffusional mass transfer at the sea floor. Limnol. Oceanogr. **38:** 52–69.

DAME, R. F. 1996. Ecology of marine bivalves. An ecosystem approach. CRC Press.

DOLMER, P. 2000. Algal concentration profiles above mussel beds. J. Sea Res. **43:** 113–119.

FRÉCHETTE, M., C. H. BUTMAN, AND W. R. GEYER. 1989. The importance of boundary-layer flows in supplying phytoplankton to the benthic suspension feeder, *Mytilus edulis* L. Limnol. Oceanogr. **34:** 19–36.

FRIEDRICHS, M., G. GRAF, AND B. SPRINGER. 2000. Skimming flow induced over a simulated polychaete tube lawn at low population densities. Mar. Ecol. Prog. Ser. **192:** 219–228.

HERMAN, P. M. J., J. J. MIDDELBURG, J. VAN DER KOPPEL, AND C. H. R. HEIP. 1999. Ecology of estuarine macrobenthos. Adv. Ecol. Res. **29:** 195–240.

JØRGENSEN, C. B. 1980. Seasonal oxygen depletion in the bottom waters of a Danish fjord and its effect on the benthic community. Oikos **34:** 68–76.

KOSEFF, J. R., J. K. HOLEN, S. G. MONISMITH, AND J. E. CLOERN. 1993. Coupled effects of vertical mixing and benthic grazing on phytoplankton populations in shallow, turbid estuaries. J. Mar. Res. **51:** 843–868.

MONISMITH, S. G., J. R. KOSEFF, J. K. THOMPSON, C. A. O'RIORDAN, AND H. M. NEPF. 1990. A study of model bivalve siphonal currents. Limnol. Oceanogr. **35:** 680–696.

MUSCHENHEIM, D. K., AND C. R. NEWELL. 1992. Utilization of seston flux over a mussel bed. Mar. Ecol. Prog. Ser. **85:** 131–136.

NILSSON, S. 2002. Flow simulation on overlapping grids, p. 544–551. *In* R. Wyrzykowski, J. Dongarra, M. Paprzycki, and J. Wasniewski [eds.], Parallel processing and applied mathematics. Proceedings of the 4th International Conference, Springer LNCS 2328.

OKUBO, A. 1980. Diffusion and ecological problems: mathematical models. Springer-Verlag.

O'RIORDAN, C. A., S. G. MONISMITH, AND J. R. KOSEFF. 1993. A study of concentration boundary-layer formation over a bed of model bivalves. Limnol. Oceanogr. **38:** 1712–1729.

———, ———, AND ———. 1995. The effect of bivalve excurrent jet dynamics on mass transfer in a benthic boundary layer. Limnol. Oceanogr. **40:** 330–344.

PATERSON, D. M., AND K. S. BLACK. 1999. Water flow, sediment dynamics and benthic biology. Adv. Ecol. Res. **29:** 155–193.

PETERSEN, J. K. 2004. Grazing on pelagic primary producers—the role of benthic suspension feeders in estuaries, p. 129–152. *In* S. L. Nielsen, G. T. Banta, and M. F. Pedersen [eds.], The influence of primary producers on estuarine nutrient cycling. Kluwer.

———, E. STENALT, AND B. W. HANSEN. 2002. Invertebrate recolonisation in Mariager Fjord (Denmark) after a severe hypoxia. II. Blue mussels (*Mytilus edulis* L.). Ophelia **56:** 215–226.

PETERSON, C. H., AND R. BLACK. 1987. Resource depletion by active suspension feeders on tidal flats: influence of local density and tidal elevation. Limnol. Oceanogr. **32:** 143–166.

RIISGÅRD, H. U., A. SUNDBERG JENSEN, AND C. JØRGENSEN. 1998. Hydrography, near-bottom currents, and grazing impact of the filter-feeding ascidian *Ciona intestinalis* in a Danish fjord. Ophelia **49:** 1–16.

ROEGNER, G. C. 1998. Hydrodynamic control of the supply of suspended chlorophyll *a* to infaunal estuarine bivalves. Estuarine Coastal Shelf Sci. **47:** 369–384.

SCHLICHTING, H. 1979. Boundary-layer theory, 7th ed. McGraw-Hill.

SOBRAL, P., AND J. WIDDOWS. 2000. Effects of increasing current velocity, turbidity and particle-size selection on the feeding activity and scope for growth of *Ruditapes decussatus* from Ria Formosa, southern Portugal. J. Exp. Mar. Biol. Ecol. **245:** 111–125.

TENNEKES, H., AND J. L. LUMLEY. 1972. First course in turbulence. MIT.

UNDERWOOD, A. J. 1996. Experiments in ecology. Cambridge Univ. Press.

WILDISH, D. J., AND D. D. KRISTMANSON. 1979. Tidal energy and sublittoral macrobenthic animals in estuaries. J. Fish. Res. Board Can. **36:** 1197–1206.

———, AND ———. 1984. Importance to mussels of the benthic boundary layers. Can. J. Fish. Aquat. Sci. **41:** 1618–1625.

———, AND ———. 1997. Benthic suspension feeders and flow. Cambridge Univ. Press.

Received: 27 May 2004
Accepted: 13 June 2005
Amended: 6 July 2005